AIAA JOURNAL
Vol. 49, No. 10, October 2011

State-Space Approach for Energy Release Rate Analysis of Delaminated Laminates with Stiffeners

Guanghui Qing,* Fengxiang Wang,† and Yanhong Liu*
Civil Aviation University of China, Tianjin 300300, People's Republic of China

DOI: 10.2514/1.J050610

Based upon the interfacial spring-layer model, a state-space approach for the energy release rate analysis of stiffened laminates with a planar delamination was presented. The main advantages of the present method are that the same mesh is used for each layer, and only the so-called state variables at the top and bottom surfaces of structure in the final control equation of structures are involved. On the other hand, the oscillatory singular stresses around the delamination front are avoided as a result. Instead, stress resultant jumps are found in the sublaminate across the delamination front. Moreover, the technique accounts for the compatibility of displacements and stresses between layers and the transverse shear deformation in the control equation of structure. To avoid the possibility of material penetration phenomenon of the delaminated region, the unilateral frictionless contact interface is adopted in the interfacial spring layer between sublaminates. With the aid of the virtual crack closure technique, the accuracy of the method was assessed by comparing the results with existing examples. The effects of stiffeners on the distribution of the energy release modes I, II, and III of the delaminated laminates with two stiffeners were analyzed by the present method.

Nomenclature

G	=	total energy release rate
G_{I}, G_{II}, G_{III}	=	energy release rate of modes I, II, and III
$\boldsymbol{p}$	=	transverse stress vector
$\boldsymbol{q}$	=	displacement vector
u, v, w	=	displacement components along (x, y, z) coordinates
x, y, z	=	orthogonal Cartesian axes x, y, and z
Γ_p, Γ_q	=	equivalent external load vectors
σ_{xz}, σ_{yz}, σ_{zz}	=	out-plane stresses
$1/R_x$, $1/R_y$, $1/R_z$	=	stiffness parameters in the x, y, and z directions

Subscripts

i, j	=	node, submatrix index, or (x, y, z) coordinates
x, y, z	=	orthogonal Cartesian axes x, y, and z

Superscripts

bl, tl	=	bottom and top surfaces of the lower sublaminate
bu, tu	=	bottom and top surfaces of the upper sublaminate
l	=	lower sublaminate
T	=	matrix transposition
u	=	upper sublaminate

I. Introduction

DURING the past several decades, much progress in the understanding of the performance and failure of composite laminates has been made, both experimentally and theoretically. However, as far as the published theoretical methods are concerned, most of them refer to one class of variable methodology (the displacement variable or the stress variable), which falls into the Lagrangian system. If 3-D finite element methods in the Lagrangian system (it is usually displacement method) are adopted to analyze the energy release rate G_{I}, G_{II}, and G_{III} or the total G of the complex delamination front in the high gradient of stress and strain states, an appropriate mesh at the delamination front is indispensable for a very accurate solution. Therefore, the 3-D finite element method may notably increase the computational cost and become not advantageous from the engineering point of view.

To reduce the cost of computation, various plate theories were generally adopted to predict G, such as the classical plate theory, the plate theory, the laminates theory, the layerwise laminate theory, and so on. For the methods based on the classical plate theory or other plate theory, most of them are not convenient for the analysis of the individual energy release rates. On the other hand, the models based on the classical plate theory cannot account for the transverse shear deformation. Because the thickness dimension can be eliminated by integrating through the laminate thickness [1–6]. The finite element models based on the laminate theories do not have the same aspect ratio limitation as the 3-D finite element models do. However, the hypothesis commonly used in the conventional laminate theories leads to a poor representation of strains (e.g., in the thick composite laminates with dissimilar material layers [7]). The layerwise laminate theories [8–11] predict the interlaminar stresses very accurately. Furthermore, it has the advantage of all plate theories in the sense that it is a two-dimensional theory and does not suffer from aspect ratio limitations associated with 3-D finite element models. But the formidable problem in the layerwise laminate theory is that the unknowns of the structural control equation increase proportionately with the increasing number of layers, which needs strong computational efforts.

The state-space approaches of elastomechanics, which fall into the methodologies of symplectic system, has attracted the attention of a number of investigators [12–29] in recent years. The outstanding advantage of the approaches is that the thick plates/shells or the laminated plates/shells problems can be treated without any displacements and stresses assumptions. The state-space approach dealing with the interlaminar continuity is different from the Zig-Zag strategies (i.e., Lekhnitskii laminated theory, Ambartsumian laminated theory and Reissner laminated theory [30]) or other refinements of classical models. Because of the transfer matrix technique being employed, the solution of the model in the state-space approaches can provide the exact continuous transverse stresses field across the thickness of laminated plate or shell structures and the order of the

Received 10 May 2010; revision received 26 February 2011; accepted for publication 17 May 2011.

*Assistant Professor, College of Aeronautical Engineering, Jinbei Road 2898.
†M.S. Student, College of Aeronautical Engineering, Jinbei Road 2898.

final governing equation system is independent of the thickness and the number of layers of such structures.

It can be seen from the published works that [31] is the first paper studied the initiation and propagation of transverse cracking in composite laminates based on the state-space approach.

By combining the interfacial spring-layer model, a state-space approach based on [7,16,20–24,28,29] has been developed to analyze the individual energy release rates of the delaminated composite laminates with stiffeners in this paper.

II. Model of Sublaminate and Interfacial Spring Layer

Figure 1 shows a delaminated laminate with two stiffeners and the delamination in plane divides the structure into two sublaminates which are called the upper sublaminate (including stiffeners) and the lower sublaminate.

Because the detailed steps for the control equation of a laminate via state-space approach can be found in [16,20–25], we only demonstrate the main steps in the present paper.

1) Assume that the four-node quadrilateral element in x-y plane [16,20–25] and the identical mesh are adopted in the each layer of a laminate.

2) Assume that the assemblage from the four-node quadrilateral element to the level of a layer is made in the usual method.

3) The dimension in the thickness direction of the assembled equation of a layer can then be eliminated by integrating operation.

4) On the basis of the interlaminar compatibility condition (including displacements and stresses) of each layer, the recurrence formulation can be used to construct the control equation of a laminate. As far as the control equation of a laminate with stiffeners is concerned, the special method can be found in [23,24].

In what follows, we simply use the following two forms to express the control equations of the upper sublaminate and lower sublaminate via the state-space approach, respectively.

For the lower sublaminate [16,20–25],

$$\begin{Bmatrix} \boldsymbol{p}^{bl} \\ \boldsymbol{q}^{bl} \end{Bmatrix} = \begin{bmatrix} \boldsymbol{T}^{l}_{11} & \boldsymbol{T}^{l}_{12} \\ \boldsymbol{T}^{l}_{21} & \boldsymbol{T}^{l}_{22} \end{bmatrix} \begin{Bmatrix} \boldsymbol{p}^{tl} \\ \boldsymbol{q}^{tl} \end{Bmatrix} + \begin{Bmatrix} \Gamma^{l}_{p} \\ \Gamma^{l}_{q} \end{Bmatrix} \tag{1a}$$

For the upper sublaminate with stiffeners (see [23,24]),

$$\begin{Bmatrix} \boldsymbol{p}^{bu} \\ \boldsymbol{q}^{bu} \end{Bmatrix} = \begin{bmatrix} \boldsymbol{T}^{u}_{11} & \boldsymbol{T}^{u}_{12} \\ \boldsymbol{T}^{u}_{21} & \boldsymbol{T}^{u}_{22} \end{bmatrix} \begin{Bmatrix} \boldsymbol{p}^{tu} \\ \boldsymbol{q}^{tu} \end{Bmatrix} + \begin{Bmatrix} \Gamma^{u}_{p} \\ \Gamma^{u}_{q} \end{Bmatrix} \tag{1b}$$

where

$$\boldsymbol{p} = [\sigma_{xz1} \;\; \sigma_{xz2} \;\; \cdots \;\; \sigma_{xzn} \;\; \sigma_{yz1} \;\; \sigma_{yz2} \;\; \cdots \;\; \sigma_{xz1} \;\; \sigma_{zz1} \;\; \sigma_{xz2} \;\; \cdots \;\; \sigma_{zzn}]^T,$$

$$\boldsymbol{q} = [u_1 \;\; u_2 \;\; \cdots \;\; u_n \;\; v_1 \;\; v_2 \;\; \cdots \;\; v_n \;\; w_1 \;\; w_2 \;\; \cdots \;\; w_n]^T$$

Superscripts bu, tu, bl, and tl denote the bottom and top surfaces of upper and lower sublaminates, respectively. $\boldsymbol{T}^{u}_{ij}$ and $\boldsymbol{T}^{l}_{ij}$ (subscripts $i, j = 1, 2$) are the equivalent stiffness matrices of the upper and lower sublaminates, respectively. They are derived from the assembled equation of each layer by integrating operation in the thickness direction and the recurrence operation between layers of the upper and lower sublaminates (see [16,20–25]). $[\Gamma^{u}_{p} \;\; \Gamma^{u}_{q}]^T$ and $[\Gamma^{l}_{p} \;\; \Gamma^{l}_{q}]^T$ are the equivalent external load vectors of the upper and lower sublaminates.

It should be pointed out that Eqs. (1a) and (1b) are the relationships of the physics quantities of top and bottom surface of the upper and lower sublaminates, respectively. As a matter of fact, Eqs. (1a) and (1b) is a set of linear algebraic equation relating to the surface nodal displacements and stresses of the upper laminate or lower laminate with stiffeners. It is obvious that the number of nodes of a layer determines the number of variables of Eq. (1). Assuming the number of nodes of a layer is n, no matter how many layers are considered, the number of variables of Eq. (1a) or Eq. (1b) is always $n \times s$ ($s = 6$, the degrees of freedom per node). On the other hand, the control equation of the each layer of the sublaminates are derived from the three-dimensional constitutive relationships [16,20–25] of material; hence, the shear effect is accounted for in all control equations of the upper and lower sublaminates.

Because Eqs. (1a) and (1b) include two group variables (namely, the stresses and displacements of structural surfaces), we cannot simply employ the interfacial constitutive relationships, which is presented in [7], to construct the whole model of a delaminated laminate with stiffeners.

In [28,29], the following interfacial linear-layer model is employed to describe the behavior of imperfection bonding between the upper and lower sublaminates:

$$\sigma^{tl}_{xz} = \sigma^{bu}_{xz} = [u^{ti} - u^{bu}]/R_x \qquad \sigma^{tl}_{yz} = \sigma^{bu}_{yz} = [v^{ti} - v^{bu}]/R_y$$
$$\sigma^{tl}_{zz} = \sigma^{bu}_{zz} = [w^{ti} - w^{bu}]/R_z \tag{2}$$

where σ^{tl}_{xz}, σ^{tl}_{yz}, σ^{tl}_{zz}, σ^{bu}_{xz}, σ^{bu}_{yz}, and σ^{bu}_{zz} refer to the stresses of the top surface of the lower sublaminate and the bottom surface of the upper sublaminate, respectively. u^{tl}, v^{tl}, w^{tl}, u^{bu}, v^{bu}, and w^{bu} denote the displacements of the top surface of the lower sublaminate and the bottom surface of the upper sublaminate, respectively. $1/R_x$, $1/R_y$, and $1/R_z$ are three stiffness parameters in the x, y, and z directions. Obviously, $R_i \to 0 (i = x, y, z)$ corresponds to a perfect bonding, while $R_i \to \infty (i = x, y, z)$ implies a completely delaminated case.

To avoid the penetration phenomenon of the completely delaminated region in present model, the technology presented in [7] is used. The unilateral frictionless contact interface is adopted by specifying a positive stiffness for closing relative displacements [7]:

$$1/R_z = \tfrac{1}{2}(1 - \text{sign}(w^{tl} - w^{bu}))k_z \quad \text{if } (w^{tl} - w^{bu}) < 0 \tag{3}$$

where k_z is a large value relative to the adjacent structure for closed stiffness. Hence, for the contact interface of the completely delaminated region [7],

$$\sigma^{tl}_{zz} = \sigma^{bu}_{zz} = \tfrac{1}{2}(1 - \text{sign}(w^{tl} - w^{bu}))k_z(w^{tl} - w^{bu}) \tag{4}$$

It is assumed that the spring layer with n nodes has the same mesh for each layer of sublaminates, the matrix form of Eq. (2) related to the node set us in the undelaminated region and the node set ds in the completely delaminated region can be simply expressed as

$$\begin{Bmatrix} \boldsymbol{p}^{tl} \\ \boldsymbol{q}^{tl} \end{Bmatrix} = \begin{bmatrix} \boldsymbol{I} & \boldsymbol{0} \\ \boldsymbol{R} & \boldsymbol{I} \end{bmatrix} \begin{Bmatrix} \boldsymbol{p}^{bu} \\ \boldsymbol{q}^{bu} \end{Bmatrix} \tag{5}$$

where

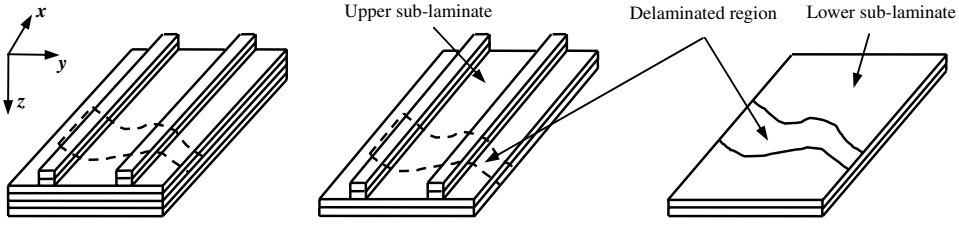

Fig. 1 Delaminated laminate with two stiffeners and coordinate system.

$$\boldsymbol{I} = \mathrm{Diag}(1)_{3n\times 3n}$$
$$\boldsymbol{R} = \mathrm{Diag}(R_{x1}\ \ R_{x2}\ \cdots\ R_{xn}\ \ R_{yn}\ \ R_{y2}\ \cdots\ R_{yn}\ \ R_{z1}\ \ R_{z2}\ \cdots\ R_{zn})$$
$$\boldsymbol{R}_{ij} = 0(i = x, y, z, j \in us)$$

Furthermore, we can also consider the soft-contact case of delaminated region. The equations for soft contact of delaminated region were presented by Bruno et al. [7]:

$$\begin{aligned} R_{zj} &= \frac{h}{2E} \quad \text{if } (w_j^{tl} - w_j^{bu}) < 0 (j \in ds) \\ R_{zj} &\to \infty \quad \text{if } (w_j^{tl} - w_j^{bu}) \geq 0 (j \in ds) \end{aligned} \tag{6}$$

where E_{33} is the elastic modulus of the z direction, and h is the thickness of the laminate.

It is not difficult to note the conclusion that Eq. (5) is a nonlinear constitutive relationship between the upper and lower sublaminates, whose dimensions are determined by the node number of the upper and lower sublaminates. However, if there does not exist a delamination region between the upper and lower sublaminates, Eq. (5) can be simplified as a linear constitutive relationship, and the coefficient matrix of Eq. (5) may also be regarded as a unit matrix.

III. Whole Model of a Delaminated Laminate with Stiffeners

In what follows, the global model of a delaminated laminate with stiffeners in terms of Eqs. (1) and (5) is reduced.

Substitution Eq. (5) into Eq. (1a), one has

$$\begin{Bmatrix} \boldsymbol{p}^{bl} \\ \boldsymbol{q}^{bl} \end{Bmatrix} = \begin{bmatrix} \boldsymbol{T}_{11}^{l} & \boldsymbol{T}_{12}^{l} \\ \boldsymbol{T}_{21}^{l} & \boldsymbol{T}_{22}^{l} \end{bmatrix} \begin{bmatrix} \boldsymbol{I} & \boldsymbol{0} \\ \boldsymbol{R} & \boldsymbol{I} \end{bmatrix} \begin{Bmatrix} \boldsymbol{p}^{bu} \\ \boldsymbol{q}^{bu} \end{Bmatrix} + \begin{Bmatrix} \Gamma_p^l \\ \Gamma_q^l \end{Bmatrix} \tag{7}$$

Then, eliminating the vector $[\,\boldsymbol{p}^{bu} \quad \boldsymbol{q}^{bu}\,]^T$ of Eq. (7) by Eq. (1b), the finally control equation of a laminate with a delamination is

$$\begin{Bmatrix} \boldsymbol{p}^{bl} \\ \boldsymbol{q}^{bl} \end{Bmatrix} = \begin{bmatrix} \boldsymbol{E}_{11} & \boldsymbol{E}_{12} \\ \boldsymbol{E}_{21} & \boldsymbol{E}_{22} \end{bmatrix} \begin{Bmatrix} \boldsymbol{p}^{tu} \\ \boldsymbol{q}^{tu} \end{Bmatrix} + \begin{Bmatrix} \boldsymbol{\Theta}_p \\ \boldsymbol{\Theta}_q \end{Bmatrix} \tag{8}$$

where

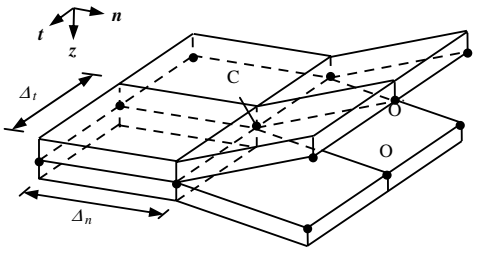

Fig. 2 Element definition and the local coordinate system [7].

$$\begin{bmatrix} \boldsymbol{E}_{11} & \boldsymbol{E}_{12} \\ \boldsymbol{E}_{21} & \boldsymbol{E}_{22} \end{bmatrix} = \begin{bmatrix} \boldsymbol{T}_{11}^{l} & \boldsymbol{T}_{12}^{l} \\ \boldsymbol{T}_{21}^{l} & \boldsymbol{T}_{22}^{l} \end{bmatrix} \begin{bmatrix} \boldsymbol{I} & \boldsymbol{0} \\ \boldsymbol{R} & \boldsymbol{I} \end{bmatrix} \begin{bmatrix} \boldsymbol{T}_{11}^{u} & \boldsymbol{T}_{12}^{u} \\ \boldsymbol{T}_{21}^{u} & \boldsymbol{T}_{22}^{u} \end{bmatrix}$$
$$\begin{Bmatrix} \boldsymbol{\Theta}_p \\ \boldsymbol{\Theta}_q \end{Bmatrix} = \begin{bmatrix} \boldsymbol{T}_{11}^{l} & \boldsymbol{T}_{12}^{l} \\ \boldsymbol{T}_{21}^{l} & \boldsymbol{T}_{22}^{l} \end{bmatrix} \begin{bmatrix} \boldsymbol{I} & \boldsymbol{0} \\ \boldsymbol{R} & \boldsymbol{I} \end{bmatrix} \begin{Bmatrix} \Gamma_p^u \\ \Gamma_q^u \end{Bmatrix} + \begin{Bmatrix} \Gamma_p^l \\ \Gamma_q^l \end{Bmatrix}$$

Obviously, Eq. (8) is formally consistent with Eq. (1a) or Eq. (1b). No matter how many layers of a laminate with a delamination are involved, Eq. (8) is of the same scale; namely, only the so-called state variables at the top surface of the upper sublaminate and bottom surfaces of the lower sublaminate are involved. Because of the contact problem involved in present model, the Newton–Raphson scheme is needed to solve Eq. (8).

IV. Calculation of Energy Release Rate

To evaluate the individual energy release rate of the delamination front numerically by the virtual crack closure technique, the G_{I}, G_{II}, and G_{III} in the local coordinate system can be expressed approximately [7]:

$$G_{\mathrm{I}} = \frac{1}{2}\frac{F_z^z \Delta w}{\Delta n \Delta t}, \qquad G_{\mathrm{II}} = \frac{1}{2}\frac{F_x^n \Delta u^n}{\Delta n \Delta t}, \qquad G_{\mathrm{III}} = \frac{1}{2}\frac{F_y^t \Delta u^t}{\Delta n \Delta t} \tag{9}$$

where F_z^z is the reaction in the spring element connecting node C in z direction, Δw is the relative z displacement between the nodes O and O', located immediately ahead the delamination front along its normal direction passing through C (see Fig. 2). Similar definitions apply for reactions F_x^n and F_y^t in the local coordinate system and relative displacement related to mode G_{II} and G_{III}. Assume that Δu^n and Δu^t are the relative x and y displacements between the nodes O and O' in the local coordinate system, respectively. The relationship between F_x^n, F_y^t, Δu^n, and Δu^t in the local coordinate system and F_x, F_y, Δu, and Δv in the global coordinate system is

$$\begin{bmatrix} F_x^n & \Delta u_n \\ F_y^t & \Delta v_t \end{bmatrix} = \begin{bmatrix} n_x & n_y \\ -n_y & n_x \end{bmatrix} \begin{bmatrix} F_x & \Delta u \\ F_y & \Delta v \end{bmatrix} \tag{10}$$

where n_x and n_y are the direction cosine.

V. Numerical Examples and Discussions

A. Example 1

First, the energy release rate G_{I} of two double cantilever beam (DCB) specimens with a straight delamination front are analyzed by the present method. One of them is made of the isotropic material: $E = 71$ GPa and Poisson's ratio $v = 0.3$. Another is made of orthotropic material: $E_{11} = 134.4$ GPa, $E_{22} = E_{33} = 13.0$ GPa, $G_{12} = G_{13} = 6.4$ GPa, $G_{23} = 4.8$ GPa, $v_{12} = v_{13} = 0.34$, and $v_{23} = 0.35$. The geometry parameters of two DCB specimens are $B = 0.0254$ m, $a = 0.0508$ m, and $h_1 = h_2 = 0.001651$ m. The vertical load on the free end $P_v = 1.0$ N/m.

It should be mentioned that in order to avoid the numerical instabilities and make sure the convergence of energy release rate, a very large value 10^8 N/mm^3 is employed to replace the $1/R_{ij} \to \infty$ of Eq. (5) in the program of all examples in this section. The value $1/R_{ij} = 10^8$ N/mm^3 corresponds to an actual approximation of the perfect adhesion condition in the normal and tangential interface, which was first suggested in the multilayer laminate model presented by Bruno et al. [7]. Bruno et al. [7] pointed out that the mesh

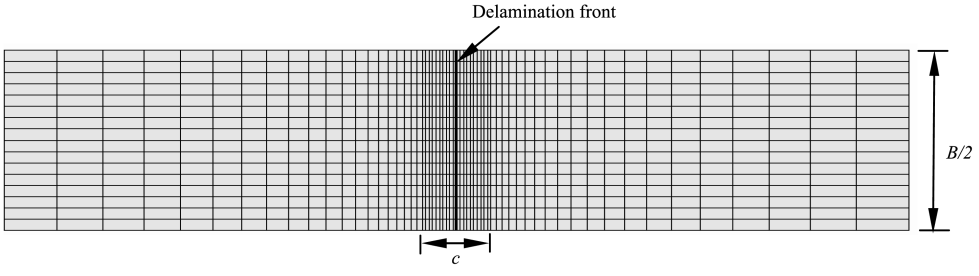

Fig. 3 Four-node quadrilateral element in *x-y* plane [16,20–25] scheme of one-half of the model.

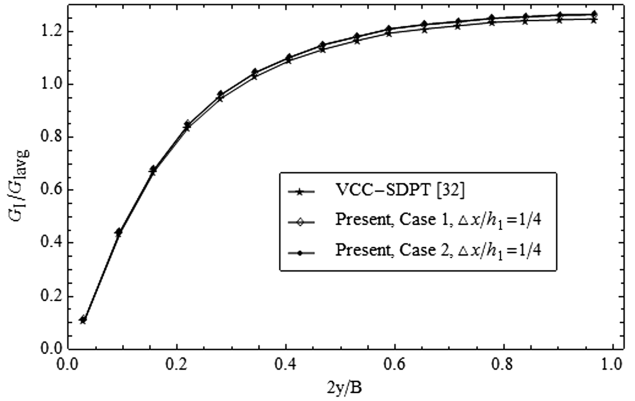

Fig. 4 Distribution of G_I for an isotropic DCB specimen (vertical load).

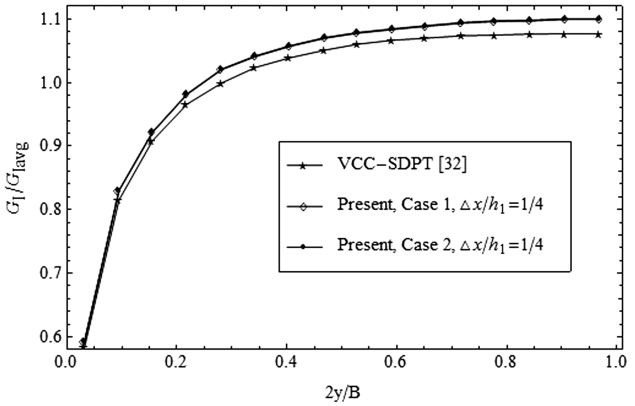

Fig. 5 Distribution of G_I for an orthotropic DCB specimen (vertical load).

refinement and convergence studies on the behavior of energy release rates as the stiffness parameters approach infinity have been conducted showing that the choice of the same value for the normal and tangential interface stiffness equal to 10^8 N/mm^3 is appropriate. The same works are carried out in our examples.

It should also be pointed out that the same mesh is adopted for all the layer and interfacial spring-layer models in the thickness direction to enable interface elements to be placed between the lower and upper sublaminates. And the fine meshing is used at the delamination front (as shown in Fig. 3).

To survey the convergence of present method, the variable delamination-front element sizes $\Delta x/h_1 = 5/10, 5/15, 5/18$, and 1/4 are employed in section c (c is approximately equal to 0.01 m, as shown in Fig. 3). The element sizes Δx of other sections are decreased as the elements come close to the section c. The number of elements across one-half of the width is 16. In the thickness direction, two cases are considered in the verification study. Case 1 is the two sublayers across the thickness of subbeams and case 2 is three sublayers across the thickness of subbeams.

It is noted that as the Δx decreases, the energy release rate G_I is slightly increased for case 1 and case 2. But the results are virtually the same for $\Delta x/h_1 = 5/18$ and 1/4, For the isotropic DCB, $G_{I\max} = 11.68 \times 10^{-5}$ J/m and $G_{I\,avg} = 9.90 \times 10^{-5}$ J/m. The maximum deviation between the results of [32] and the present method is 1.4%: De = (RP − RR)/RR × 100, where De is the deviation, RP is the results of the present method, and RR is the results of [32]. $G_{I\,avg}$ is determined by summing the values of G_I for each element and dividing by the number of elements across the width (Fig. 4). It is suggested that three sublayers across the thickness of subbeams and the delamination-front element size $\Delta x/h_1 = 1/4$ are sufficient to obtain the converged results in this example. Certainly, the thickness ratio of structures is a sensitive parameter in relation to the solution of the state-space equation. If the thickness ratio is greater than that of our examples, more sublayers across the thickness of subbeams may be necessary.

Table 1 Material parameters, dimensions, and loads

Parameters	Values
Upper and lower sublaminates, GPa	
E_{11}	139.4
E_{22}	10.16
E_{33}	10.16
G_{12}	4.6
G_{13}	4.6
G_{23}	3.54
v_{12}	0.3
v_{13}	0.3
v_{23}	0.436
Dimensions, m	
L	0.12
a	0.06
h_1	0.001
h_2	0.0015
B	0.04
B_1	0.02
w	0.004
Load, N/m	
P_v	1
P_t	1

The G_I distribution of orthotropic DCB is shown in Fig. 5. Comparing with the result reported in [32], the maximum deviation is 1.6%.

It is very interesting that in our example, with dimension in the thickness direction eliminated of sublaminates via integrating operation of each layer and the recurrence operation between layers, there is no mechanism to accommodate stress singularity [7,33–35] around the delamination front, the oscillatory behavior is not present. Instead, there exist stress resultant discontinuities across the delamination front reflecting the effect of the singularity.

B. Example 2

Consider a laminated beam [0°/0°/90°/0°] with two stiffeners (Fig. 6). The laying angle of stiffeners is 0°. The material parameters, dimensions, and loads are given in Table 1.

The refined element in the x-y plane is similar to two examples above. The number of elements across B, B_1, and w is 40, 16, and 8, respectively. The number of sublayers of the upper sublaminate and lower sublaminate are 2 and 3, respectively. Five models (namely, $h_s = 0.0000$ m, $h_s = 0.0005$, 0.001, 0.0015, and 0.0020 m) are analyzed for the delamination-front element sizes $\Delta x/h_1 = 1/4$. As we expected, the distribution of G_I for the vertical load on the free end are basically the same when $\Delta x/h_1 = 5/18$ and 1/4.

As show in Fig. 7, the distribution of G_I is dependent on the stiffeners for the vertical load on the free end. The G_I values on the area of stiffeners are greater than other area. The maximum value G_I is found in the center of the area of stiffeners and then drops down. The effect of the stiffeners on the distribution of G_I is more pronounced when the thickness of stiffeners is larger.

In what follows, the contact and no contact analysis are carried out for a tear load on the free end. In particular, the soft-contact constitutive relationships [7] are considered.

Figures 8 and 9 show that the distribution of G_I between contact analysis and no contact analysis are noticeably different for the tear

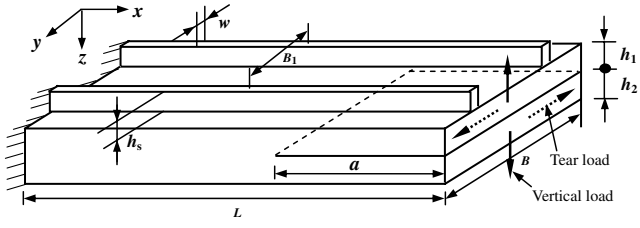

Fig. 6 Laminated beam.

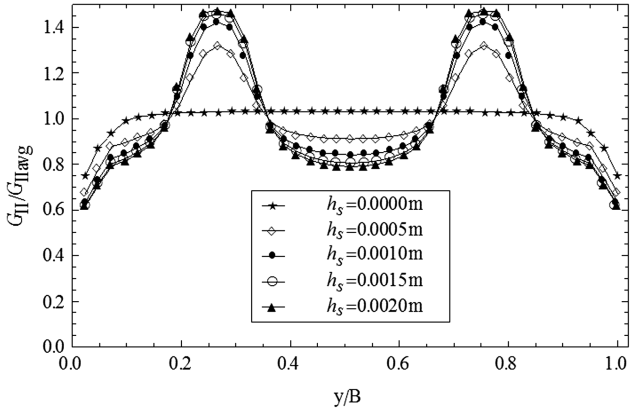

Fig. 7 Distribution of G_I for composite laminates with two stiffeners (vertical load).

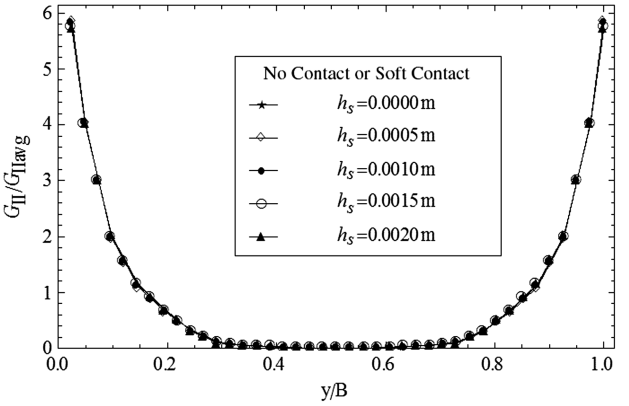

Fig. 10 Distribution of G_{II} for a composite laminate with two stiffeners (tear load).

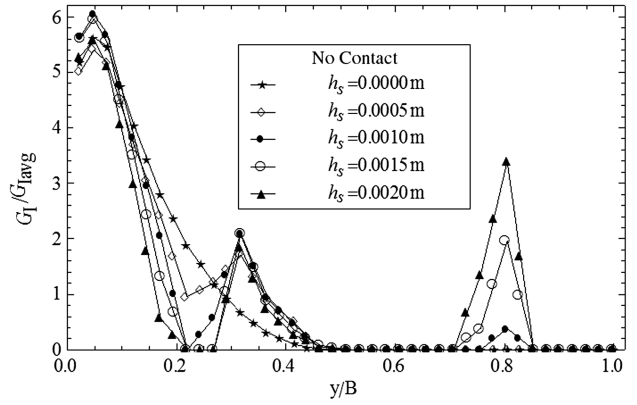

Fig. 8 Distribution of G_I for a composite laminate with two stiffeners (tear load).

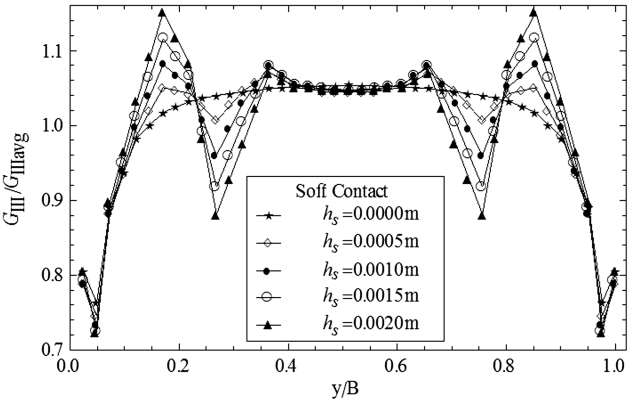

Fig. 11 Distribution of G_{III} for a composite laminate with two stiffeners (tear load).

load case, whereas the G_{II} and G_{III} (Figs. 10 and 11) are basically the same. Therefore, if we want to obtain the reliable G_I relative to the tear load, a contact analysis is inevitable.

It is also evident that for the tear load case, the distribution of G_I is also dependent on the stiffeners and the value G_I at the area of stiffeners are greater in contrast to the adjacent area. As the height of stiffeners is increased, the G_I values are on the increase in the area of free edge (Figs. 8 and 9). The effect of stiffeners on the distribution of G_{II} along the width are insignificant (Fig. 10).

As can be seen from Figs. 7–9 and 11, due to the existing stiffeners, the distribution of G_I on the vertical or tear load and the distribution of G_{III} on the tear load become a bit more complicated. And the stiffeners seem to be unfavorable for the distribution of G_I and G_{III} in our examples above.

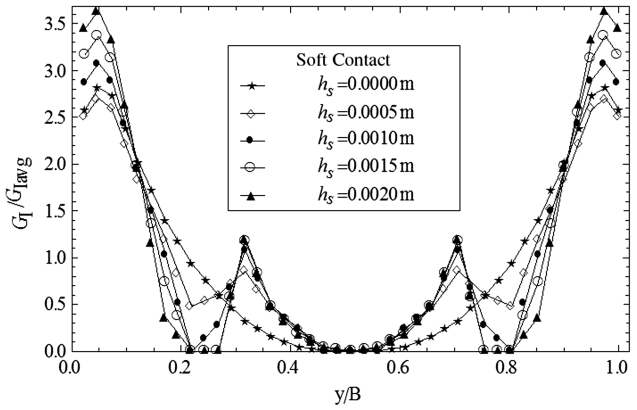

Fig. 9 Distribution of G_I for a composite laminate with two stiffeners (tear load).

VI. Conclusions

In this paper, by adopting an interfacial spring layer based on fracture and contact mechanics, a state-space approach for the analysis of energy release rates of delaminated laminates with stiffeners has been presented. In accordance with its physical configuration, the laminate is modeled as an assembly of three-dimensional layers connected by the transfer matrix technique in the transverse direction. The soft-contact model is used to simulate contact between delaminated members.

First, the model is applied to compute the energy release rate G_I of two double cantilever beam specimens with a through-the-width delamination. The results obtained are compared with those in published works. And then the effect of stiffeners on the distribution of the energy release modes I, II, and III are investigated by simulating a delaminated laminate with two stiffeners.

Based upon the mathematical model presented in this paper, the following remarks can made:

1) The mesh in the model is used only in the two-dimensional plane and the number of variables of the final control equation via the state-space approach is independent of the thickness and the layer numbers of the laminates; therefore. the proposed model results in a lower computational cost in comparison with some full three-dimensional FE models.

2) The model accounts for the transverse shear deformation, because the control equations of sublaminates are derived from the three-dimensional constitutive relationships [16,20–25].

3) The interfacial spring layer between the upper and lower sublaminates is consistent with the physical behavior of continuous transverse stresses and displacements in the undelaminated region by specifying the large values of springs and avoids the possibility of material penetration phenomenon in the delaminated region by using the soft-contact constitutive relationships.

4) The interfacial spring layer with zero thickness can be operated as a simple transfer matrix to establish the control equation of whole structure.

5) On the other hand, in the proposed model, the oscillatory singular stresses around the delamination front are avoided due to the exclusion of deformability in the thickness direction of sublaminate via integrating operation of each layer and the recurrence operation between layers. Instead, stress resultant jumps are lumped into concentrated forces by interfacial spring layer with zero thickness. This advantage is the same as in [7].

6) Certainly, the present approach is a simple yet powerful alternative to simulate the multiple delaminations problems of the composite structures.

Acknowledgment

This work was supported by the Natural Science Foundation of Tianjin (grant no. 07JCYBJC02100), People's Republic of China.

References

[1] Williams, J. G., "On the Calculation of Energy Release Rates for Cracked Laminates," *International Journal of Fracture*, Vol. 36, No. 2, 1988, pp. 101–119. doi:10.1007/BF00017790

[2] Suo, Z., and Hutchinson, J. W., "Interface Crack Between Two Elastic Layers," *International Journal of Fracture*, Vol. 43, No. 1, 1990, pp. 1–18. doi:10.1007/BF00018123

[3] Toya, M., Aritomi, M., and Chosa, A., "Energy Release Rates for an Interface Crack Embedded in a Laminated Beam Subjected to Three Point Bending," *Journal of Applied Mechanics*, Vol. 64, No. 2, 1997, pp. 375–382. doi:10.1115/1.2787318

[4] Sheinman, I., and Kardomateas, G. A., "Energy Release Rate and Stress Intensity Factors for Delaminated Composite Laminates," *International Journal of Solids and Structures*, , Vol. 34, No. 4, 1997, pp. 451–459. doi:10.1016/S0020-7683(96)00018-2

[5] Zou, Z., Reid, S. R., Soden, P. D., and Li, S., "Mode Separation of Energy Release Rate for Delamination in Composite Laminated Using Sublaminates," *International Journal of Solids and Structures*, Vol. 38, No. 15, 2001, pp. 2597–2613. doi:10.1016/S0020-7683(00)00172-4

[6] Altus, E., and Dorogoy, A., "A Three-Dimensional Study of Delamination," *Engineering Fracture Mechanics*, Vol. 33, No. 1, 1989, pp. l–19.

[7] Bruno, D., and Greco, F., "A 3D Delamination Modelling Technique Based on Plate and Interface Theories for Laminated Structures," *European Journal of Mechanics, A/Solids*, Vol. 24, No. 1, 2005, pp. 127–149. doi:10.1016/j.euromechsol.2004.11.005

[8] Barbero, E. J., and Reddy, J. N., "Modeling of Delamination in Composite Laminates Using a Layerwise Plate Theory," *International Journal of Solids and Structures*, , Vol. 28, No. 3, 1991, pp. 373–388. doi:10.1016/0020-7683(91)90200-Y

[9] Robbins, D. H., Reddy, J. N., and Krishna Murty, A. V., "On the Modeling of Delamination in Thick Composites," *Enhancing Analysis Techniques for Composite Materials*, Vol. 10, ASME International, New York, 1991, pp. 133–149.

[10] Lee, J., Gurdal, Z., and Griffin, O. J., "Layerwise Approach for the Bifurcation Problem in Laminated Composites With Delaminations," *AIAA Journal*, Vol. 31, No. 2, 1993, pp. 331–338. doi:10.2514/3.11672

[11] Gilat, R., Williams, T. O., and Aboudi, J., "Buckling of Composite Plates by Global-Local Plate Theory," *Composites, Part B*, Vol. 32, No. 3, 2001, pp. 229–236. doi:10.1016/S1359-8368(00)00059-7

[12] Chandrashekara, S., and Santhosh, U., "Natural Frequencies of Cross-Ply Laminates by State Space Approach," *Journal of Sound and Vibration*, Vol. 136, No. 3, 1990, pp. 413–424. doi:10.1016/0022-460X(90)90453-7

[13] Fan, J. R., and Ye, J. Q., "A Series Solution of the Exact Equation for Thick Orthotropic Plates," *International Journal of Solids and Structures*, , Vol. 26, No. 7, 1990, pp. 773–778. doi:10.1016/0020-7683(90)90006-H

[14] Steele, C. R., and Kim, Y. Y., "Modified Mixed Variational Principle and the state-Vector Equation for Elastic Bodies and Shells of Revolution," *Journal of Applied Mechanics*, Vol. 59, No. 3, 1992, pp. 587–595. doi:10.1115/1.2893764

[15] Heyliger, P. R., and Brooks, P., "Free Vibration of Piezoelectric Laminates in Cylindrical Bending," *International Journal of Solids and Structures*, , Vol. 32, No. 20, 1995, pp. 2945–2959. doi:10.1016/0020-7683(94)00270-7

[16] Zou, G. P., and Tang, L. M., "A Semi-Analytical Solution for Laminated Composite Plates in Hamilton System," *Computer Methods in Applied Mechanics and Engineering*, Vol. 128, Nos. 3–4, 1995, pp. 395–404. doi:10.1016/0045-7825(95)00877-2

[17] Ting, T. C., *Anisotropic Elasticity Theory and Application*, Oxford Univ. Press, New York, 1996, Chaps. 2, 3.

[18] Ding, H. J., Chen, W. Q., and Xu, R. Q., "New State Space Formulations for Transversely Isotropic Piezoelectricity with Application," *Mechanics Research Communications*, Vol. 27, No. 3, 2000, pp. 319–326. doi:10.1016/S0093-6413(00)00098-7

[19] Tarn, J. Q., "A state space formalism for piezothermmoelasticity," *International Journal of Solids and Structures*, , Vol. 39, No. 20, 2002, pp. 5173–5184. doi:10.1016/S0020-7683(02)00413-4

[20] Sheng, H. Y., and Ye, J. Q., "A Semi-Analytical Finite Element for Laminated Composite Plates," *Composite Structures*, Vol. 57, No. 1, 2002, pp. 117–123. doi:10.1016/S0263-8223(02)00075-2

[21] Sheng, H. Y., and Ye, J. Q., "A Three-Dimensional State Space Finite Element Solution for Laminated Composite Cylindrical Shells," *Computer Methods in Applied Mechanics and Engineering*, Vol. 192, Nos. 22–23, 2003, pp. 2441–2459. doi:10.1016/S0045-7825(03)00265-2

[22] Zhong, W. X., *Symplectic System of Applied Mechanics*, Science Press, Beijing, 2003, Chaps. 4–8 (in Chinese).

[23] Qing, G. H., Qiu, J. J., and Liu, Y. H., "Free Vibration Analysis of Stiffened Laminated Plates," *International Journal of Solids and Structures*, , Vol. 43, No. 6, 2006, pp. 1357–1371. doi:10.1016/j.ijsolstr.2005.03.012

[24] Qing, G. H., Qiu, J. J., and Liu, Y. H., "A Semi-Analytical Solution for Dynamic Analysis of Plate with Piezoelectric Patches," *International Journal of Solids and Structures*, , Vol. 43, No. 6, 2006, pp. 1388–1403. doi:10.1016/j.ijsolstr.2005.03.048

[25] Qing, G. H., Liu, Y. H., Qiu, J. J., and Meng, X. J., "A Semi-Analytical Method for the Free Vibration Analysis of Thick Double-Shell Systems," *Finite Elements in Analysis and Design*, Vol. 42, No. 10, 2006, pp. 837–845. doi:10.1016/j.finel.2006.01.002

[26] Qing, G. H., Xu, J. X., and Qiu, J. J., "A New Efficient Numerical Method and Dynamic Analysis of Composite Laminates with Piezoelectric Layers," *Composite Structures*, Vol. 78, No. 4, 2007, pp. 457–467. doi:10.1016/j.compstruct.2005.11.002

[27] Qing, G. H., Liu, Y. H., Guo, Q., and Zhang, D. D., "Dynamic Analysis for Three-Dimensional Laminated Plates and Panels with Damping," *International Journal of Medical Sciences*, Vol. 50, No. 1, 2008, pp. 83–91. doi:10.1016/j.ijmecsci.2007.05.002

[28] Chen, W. Q., Cai, J. B., and Ye, G. R., "Exact Solutions of Cross-Ply Laminates with Bonding Imperfections," *AIAA Journal*, Vol. 41, No. 11, 2003, pp. 2244–2250. doi:10.2514/2.6817

[29] Chen, W. Q., and Lee, K. Y., "Three-Dimensional Exact Analysis of Angle-Ply Laminates in Cylindrical Bending with Interfacial Damage via State Space Method," *Composite Structures*, Vol. 64, Nos. 3–4, 2004, pp. 275–283. doi:10.1016/j.compstruct.2003.08.010

[30] Carrera, E., "Historical Review of Zig-Zag Theories for Multilayered Plates and Shells," *Applied Mechanics Reviews*, Vol. 56, No. 3, 2003, pp. 287–308. doi:10.1115/1.1557614

[31] Ye, J. Q., Lam, D., and Zhang, D. X., "Initiation and Propagation of Transverse Cracking in Composite Laminates," *Computational Materials Science*, Vol. 47, No. 4, 2010, pp. 1031–1039. doi:10.1016/j.commatsci.2009.12.003

[32] Davidson, B. D., and Schapery, R. A., "A technique for Predicting Mode I Energy Release Rates Using a First-Order Shear Deformable Plate Theory," *Engineering Fracture Mechanics*, Vol. 36, No. 1, 1990, pp. 157–165. doi:10.1016/0013-7944(90)90105-P

[33] Bruno, D., Greco, F., and Lonetti, P., "A Coupled Interface-Multilayer

Approach for Mixed Mode Delamination and Contact Analysis in Laminated Composites," *International Journal of Solids and Structures*, Vol. 40, No. 26, 2003, pp. 7245–7268. doi:10.1016/j.ijsolstr.2003.09.006

[34] Greco, F., Lonetti, P., and Nevone Blasi, P., "An Analytical Investigation of Debonding Problems in Beams Strengthened Using Composite Plates," *Engineering Fracture Mechanics*, Vol. 74, No. 3, 2007, pp. 346–372. doi:10.1016/j.engfracmech.2006.05.023

[35] Bruno, D., Carpino, R., and Greco, F., "Modelling of Mixed Mode Debonding in Externally FRP Reinforced Beams," *Composites Science and Technology*, Vol. 67, Nos. 7–8, 2007, pp. 1459–1474. doi:10.1016/j.compscitech.2006.07.019

A. Pelegri
Associate Editor